

Active matter logic for autonomous microfluidics

Francis G. Woodhouse^{1*} and Jörn Dunkel²

¹Department of Applied Mathematics and Theoretical Physics,
Centre for Mathematical Sciences, University of Cambridge,
Wilberforce Road, Cambridge CB3 0WA, U.K.

²Department of Mathematics, Massachusetts Institute of Technology,
77 Massachusetts Avenue, Cambridge MA 02139-4307, U.S.A.

*To whom correspondence should be addressed; E-mail: F.G.Woodhouse@damtp.cam.ac.uk.

Chemically or optically powered active matter plays an increasingly important role in materials design but its computational potential has yet to be explored systematically. The competition between energy consumption and dissipation imposes stringent physical constraints on the information transport in active flow networks, facilitating global optimization strategies that are not well understood. Here, we combine insights from recent microbial experiments with concepts from lattice-field theory and non-equilibrium statistical mechanics to introduce a generic theoretical framework for active matter logic (AML). Highlighting conceptual differences with classical and quantum computation, we demonstrate how the inherent non-locality of incompressible active flow networks can be utilized to construct universal logical operations, Fredkin gates and memory storage in SR latches through the synchronized self-organization of many individual network components. Our work lays the conceptual foundation for developing autonomous microfluidic transport devices driven by bacterial fluids, active liquid crystals or chemically engineered motile colloids.

Active materials^{1,2} powered by light or chemical sources offers intriguing technological and biomedical potential, from targeted drug delivery³ and microscale reactors^{4,5} to tissue engineering⁶ and energy harvesting^{7,8}. An important subgroup of active materials is fluid-based², encompassing ATP-driven liquid crystals^{9,10}, bromine-fueled squirmer droplets¹¹, Janus particles¹²⁻¹⁴, colloidal rollers¹⁵ and microbial suspensions^{16,17}. These systems are central to current microfluidic soft robotics research¹⁸ owing to their ability to self-assemble into complex structures¹²⁻¹⁴, spontaneously create unidirectional flows¹⁹ and transport microcargos^{7,20}. While much has been learned about the ordering principles of active fluid systems in the last decade², their intrinsic computational potential has yet to be systematically explored and exploited²¹⁻²³.

The recent discovery of collective bacterial spin states¹⁷ suggests that self-organized active flows can be utilized for microfluidic information storage or transport. Moreover, certain classes of organisms, such as the slime mold *Physarum polycephalum*^{24,25}, use fluid-mediated computation strategies to solve complex optimization problems, but the decentralized algorithms at work have yet to be deciphered. Microfluidic technology has been successfully employed to perform universal Boolean computation through sub-millimeter bubbles²⁶, enabling the logical control of chemical micro-reactors in lab-on-a-chip devices. However, bubble logic relies on only local hydrodynamic interactions and requires an externally applied pressure difference²⁶, analogous to an applied voltage in a conventional computer. Ferrofluid droplet computation²⁷ similarly depends on an external rotating magnetic field ‘clock’. By contrast, active liquids can flow spontaneously^{9-11,19} and exhibit non-local topological interactions²⁸. These two distinctive features make active fluids a promising candidate for the implementation of autonomous computation schemes to drive microfluidic reaction, mixing and transport devices and uncover algorithmic principles underlying decentralized decision-making in *Physarum*^{24,25} and other organisms.

The computational power of any physical or biological system is limited by design choices²⁹ and thermodynamic constraints³⁰. Classical Turing-type machines²⁹ sequentially perform localized binary operations while being energetically limited through Landauer’s principle³¹. Quantum computers³² exploit nonlocal entanglement but typically require very low operating temperatures to suppress decoherence. Neural circuits³³ rely on feedback loops that can be expensive to maintain³⁴. DNA computing^{35,36} exploits parallelism to counter slow processing speeds. The active flow networks (AFNs) considered here operate far from thermal equilibrium and realize a nonlocal computation approach that functions at room temperature by combining global incompressibility with local energy conversion constraints. The balance of energy uptake and dissipation forces a microbial or ATP-driven fluid to travel at a preferred speed along micro-channels¹⁹ while fluid incompressibility imposes topological con-

straints on the flow network dynamics that enable the implementation of logical operations. A compact mathematical description of AFNs is made possible by a recently established mapping onto an effective lattice-field theory²⁸. Here, we will use this generic framework to implement universal logical operations, reversible gates and memory storage in SR latches through the synchronized action of many individual AFN components. We will also evaluate the robustness of AFN-based computation against noise.

An AFN is defined as an oriented graph $\Gamma = (V \cup \partial\Gamma, E)$ with bulk vertices V , 1-valent boundary vertices $\partial\Gamma$ and edges E , where each $e \in E$ possesses a flux $\phi_e \in \mathbb{R}$ such that $\phi_e > 0$ and $\phi_e < 0$ represent flow with and against the orientation of e , respectively. If fluctuations can be neglected, the flow vector $\Phi = (\phi_e)$ obeys the pseudo-Hamiltonian $H = H_0 + H_{\partial\Gamma} + H_+$. The base energy H_0 reads²⁸

$$H_0 = \lambda \sum_{e \in E} V(\phi_e) + \frac{1}{2}\mu \sum_{v \in V} (\mathbf{D} \cdot \Phi)_v^2,$$

with $\mathbf{D} = (D_{ve})$ the signed incidence matrix of Γ . H_0 models spontaneous active flow $\phi_e = \pm 1$ through the double-welled potential $V(\phi_e) = -\frac{1}{4}\phi_e^4 + \frac{1}{6}\phi_e^6$ while constraining net flux $(\mathbf{D} \cdot \Phi)_v$ at each bulk vertex v to be approximately zero, provided the coupling constants λ and μ satisfy $\mu \gg \lambda$; this incompressibility constraint makes AFNs topologically distinct from conventional neural networks^{33,37}. The sextic flux potential V avoids an unphysical hidden symmetry of quartics²⁸ to yield discrete energy minima with $\phi_e \approx \pm 1$ or $\phi_e \approx 0$ ¹⁹. The boundary energy

$$H_{\partial\Gamma} = \frac{1}{2}\mu \sum_{v \in \partial\Gamma_{\text{in}}} [(\mathbf{D} \cdot \Phi)_v + I_v]^2$$

on $\partial\Gamma = \partial\Gamma_{\text{in}} \cup \partial\Gamma_{\text{out}}$ controls inputs and outputs: input vertices $\partial\Gamma_{\text{in}}$ have net outward flux according to the prescribed binary input vector $\mathbf{I} = (I_v)$, whereas output vertices $\partial\Gamma_{\text{out}}$ remain unconstrained; instead, their net flux $O_v = (\mathbf{D} \cdot \Phi)_v$ defines the output vector $\mathbf{O} = (O_v)$. (Note that since all $v \in \partial\Gamma$ are 1-valent, each v has a single unique edge to which it is incident.) Finally, the diode energy H_+ constrains any diode edges $E_+ \subseteq E$ to permit flow only in the positive direction $\phi_e > 0$, with $H_+ = \infty$ if $\phi_e < 0$ for any $e \in E_+$ and zero otherwise, as can be realized through geometric channel patterning³⁸. In particular, we always place in E_+ the (appropriately oriented) edges incident to the input and output vertices $\partial\Gamma$ to prevent spurious backflow into or out of the system.

AFNs allow us to construct logical circuits in a conceptually different fashion to traditional conservative logic³⁹. When Γ is restricted to vertices of degree at most 3, as we will do here, stable states of an incompressible AFN comprise vertex-disjoint paths from each active

input to distinct outputs and, where possible, closed vertex-disjoint cycles through other internal vertices, with the configuration energy H proportional to the (negative of the) number of flowing edges. Because these flows are disjoint, they constrain one another's allowable locations according to the global topology of Γ . Thus the behavior with one input active can be changed globally by activating a second input, suggesting that complex operations can be computed by appropriately designed networks. This is particularly true in the zero-noise limit when the only states—the ground states of H —are those with the maximum possible number of edges flowing. It is in this limit that we have the most control in order to create active logic gates, as we now show.

The elementary operations AND (\wedge) and OR (\vee) can be realized simultaneously as the ground states of a single small active network (Fig. 1a). The network accepts two inputs, X and Y , and its two outputs give $X \wedge Y$ and $X \vee Y$. This is achieved through a single cross-input coupling edge and the insertion of simple edges before one output ($X \vee Y$) to render it energetically favorable to the other ($X \wedge Y$) when only one input is active. Another elementary operation, NOT (\neg), can also be simply realized (Fig. 1b). Unlike AND/OR, since NOT must output 1 from an input of 0, flux conservation demands an additional power leg permanently fixed at 1; conversely, to output 0 for an input of 1 with power also present, conservation demands two ground legs, whose value is ignored, down which the input and power can be dumped. These concepts are familiar from traditional conservative logic³⁹.

In classical logic circuits, chaining AND and NOT yields the universal gate NAND which can be used to implement arbitrary Boolean logic. In AFNs, non-trivial global topological effects mean that naively combining active networks for AND and NOT does not necessarily yield NAND. Nevertheless, active networks can still be exploited to construct NAND in this fashion by lengthening ground legs of the naive AND-NOT concatenation, upweighting the X -to-ground path in AND to induce the desired ground states (Fig. 1c). Another departure from classical circuits is in the FAN-OUT operation or signal splitter, taking one input and replicating it on two identical outputs. Since active network flows are effectively discretized, a signal cannot be copied simply by splicing on another wire; rather, FAN-OUT is itself a powered and grounded active circuit. In fact, since X is output on both ground legs, FAN-OUT is realized simultaneously with NOT in Fig. 1b, akin to the simultaneous realization of AND and OR in Fig. 1a. This circuit can then be appended to any other gate to increase that gate's fan-out count, provided other output legs are lengthened as necessary in order to preserve the required ground state paths. In general, as in traditional conservative logic³⁹, the ground legs of an operation may output other useful logical expressions that can simplify construction of a larger system. These considerations emphasize how active matter logic (AML) is most effective as a top-down, global construction to benefit from the advantage of

autonomy inherent in AFNs.

When the AFN is coupled to an environment that acts as a heat bath, the probability of a flow configuration Φ can be approximately described in the absence of complex correlation statistics⁴⁰ by a Boltzmann weight $\propto \exp[-\beta H(\Phi)]$, where β measures the inverse noise strength. AML then becomes probabilistic with a drop-off from perfect accuracy that can be tuned through geometry or microscopic activity^{9,19}. For $\beta \gg 1$ and $\mu \gg \lambda$, the order of magnitude of the error—the probability of observing the incorrect result—can be evaluated in terms of the free-edge flow weighting $\alpha = e^{-\beta\lambda/12} \ll 1$ by replacing the continuous density of states with that of a discretized system $\Phi \in \{-1, 0, 1\}^{|E|}$ and expanding probabilities in α . This estimation shows that while the error in the NAND gate in Fig. 1c is linear in α , the AND/OR network in Fig. 1a is more robust for specific input combinations. In particular, on top of simple mass conservation demanding that AND and OR must be essentially perfect for identical inputs $X = Y$, AND exhibits error of only $O(\alpha^3)$ for $X = 0, Y = 1$. This robustness—due to the difference in the number of active edges between the two possible output states—and that of the more sensitive $X = 1, Y = 0$ input pair can be further exponentially enhanced by lengthening the upper edge, trading simplicity for accuracy. True operational error can be quantified by numerical evaluation of the marginal distribution $p(O_v|\mathbf{I})$ for the desired output vertex v , as shown for NAND in Fig. 1d by numerical integration of the Langevin equation $d\Phi = -\nabla H dt + \sqrt{2\beta^{-1}} d\mathbf{W}_t$ at two noise amplitudes. These results imply that the desired robustness and the noise characteristics of the realization scheme should be taken into account when designing AML systems.

Multistable circuits with memory arise naturally within AML as dynamic networks with multiple ground states. A classic set–reset (SR) latch requires at least two logic gates—two NANDs, for instance—and feedback loops between them. In contrast, the global topological feedback inherent in AFNs mean that a memory circuit similar to the SR latch can be constructed very simply (Fig. 2). When S and R are both 0, the two network ground states correspond to outputs $Q = 0$ and $Q = 1$. In the zero noise limit $\beta \rightarrow \infty$ these states are stable and the output will not change until one of S or R is changed. On setting S to 1, the flow route from the power leg to ground is cut off and Q immediately sets to 1; upon releasing S , the stable state requiring fewest edge changes (and so nearest in state space) will be favored²⁸ and $Q = 1$ is set. Conversely, setting R to 1 forces the power flow through the ground leg such that releasing R then favors the state with $Q = 0$. Implementing this circuit as a continuous active network obeying pseudo-equilibrium Langevin dynamics^{17,28} confirms its memory properties at low noise (Fig. 2c). Traditional SR latch behavior, where $Q = 0$ is output immediately on setting $R = 1$, would require a doubly-grounded network capable of dissipating both the power and reset signals.

The **NAND** gate in Fig. 1c is not reversible, since the $(X, Y) = (0, 1)$ and $(1, 0)$ inputs yield identical output and ground leg states: that is, the precise input state cannot be deduced from all readable output data. However, employing closed loops within an AFN, exploiting mutual exclusivity of active flows, allows fully reversible gates to be constructed. For example, a reversible **XOR** (\oplus) gate is provided by the two-output CNOT (controlled-NOT) operation familiar to quantum logic³², realized in Fig. 3a. This accepts an input X and a control signal C , outputting $\neg X$ if C is 1 and X if C is 0, which is precisely $X \oplus C$, as well as always outputting C , giving a one-to-one mapping of input pairs (X, C) to output pairs $(X \oplus C, C)$. The more complex three-input Fredkin or CSWAP gate³⁹, which is remarkably both reversible and universal, can also be realized in AML (Fig. 3b). In general, mass conservation means that we expect fully reversible computing to be realizable within the AML framework.

Beyond logical operations, finding local energy minima of an AFN can be recast as a Boolean satisfiability problem (SAT) similar to those considered in DNA-based computing^{35,36}. Suppose that Γ is closed—that is, it has no inputs or outputs ($\partial V = \emptyset$). To each edge flux ϕ_e we associate a Boolean variable x_e where $x_e = 1$ represents $\phi_e = \pm 1$ and $x_e = 0$ represents $\phi_e = 0$. Incompressibility at a vertex $v \in V$ then implies the logical condition that an even number of the incident edges $e \in E(v)$ have $x_e = 1$. For example, a bulk degree-3 vertex with incident edge variables x_1, x_2, x_3 has incompressibility condition

$$(\neg x_1 \vee \neg x_2 \vee \neg x_3) \wedge (\neg x_1 \vee x_2 \vee x_3) \wedge (x_1 \vee \neg x_2 \vee x_3) \wedge (x_1 \vee x_2 \vee \neg x_3)$$

in conjunctive normal form. Combining vertices then yields a k -SAT problem, where k is the maximum vertex degree in Γ , whose solutions are potential metastable states of H . If Γ contains no dioded (one-way) edges then these are all energy minima, with multiplicity determined by the number of orientations of the subgraph induced by those $e \in E$ with $x_e = 1$; if there are multiple dioded edges, then some logical states may not be orientable. Input and output vertices simply add further logical conditions: the former force edges to assume 1 or 0 values according to the input vector \mathbf{I} , and the dioded edges of the latter reduce to fixing the number of 1-valued output edges to be the number of inputs. In general, many active biological network processes might be fruitfully cast in logical terms: *P. polycephalum*, for instance, could be viewed as solving a constrained SAT problem to coarsen an initially fine foraging network^{24,25}.

AFNs present a flexible framework for biologically-rooted computing and autonomous lab-on-a-chip devices. The global topological coupling core to their construction lends AML interesting advantages over classical computing. For instance, eavesdropping detection be-

comes near-trivial, since any snooping device installed within the network—or even on an ignored ground leg—is likely to fundamentally alter the ground states of the AFN, changing the output behavior and rendering the intrusion obvious. The technology to implement AFN-based logic devices is now becoming available: electrostatically-driven colloids^{13,15}, self-propelled droplets¹¹, polar microfilaments⁴¹, artificial extensile nematics⁹ and microswimmer suspensions^{17,19,38,42} all present feasible AML realization schemes capable of sustaining microfluidic matter transport, which may yield even richer behavior when coupled with additional external control mechanisms such as optical activation⁴³ or chemical patterning^{4,44}. Fully exploiting the global character of these systems to construct arbitrary computation will require innovative coupling of techniques from statistical physics, control theory and graph theory, lending insight into the natural optimization strategies that underly the balance between energy consumption and dissipation constraints present in biological systems.

Acknowledgements This work was supported by Trinity College, Cambridge (F.G.W.), an Alfred P. Sloan Research Fellowship (J.D.), and an Edmund F. Kelly Research Award (J.D.).

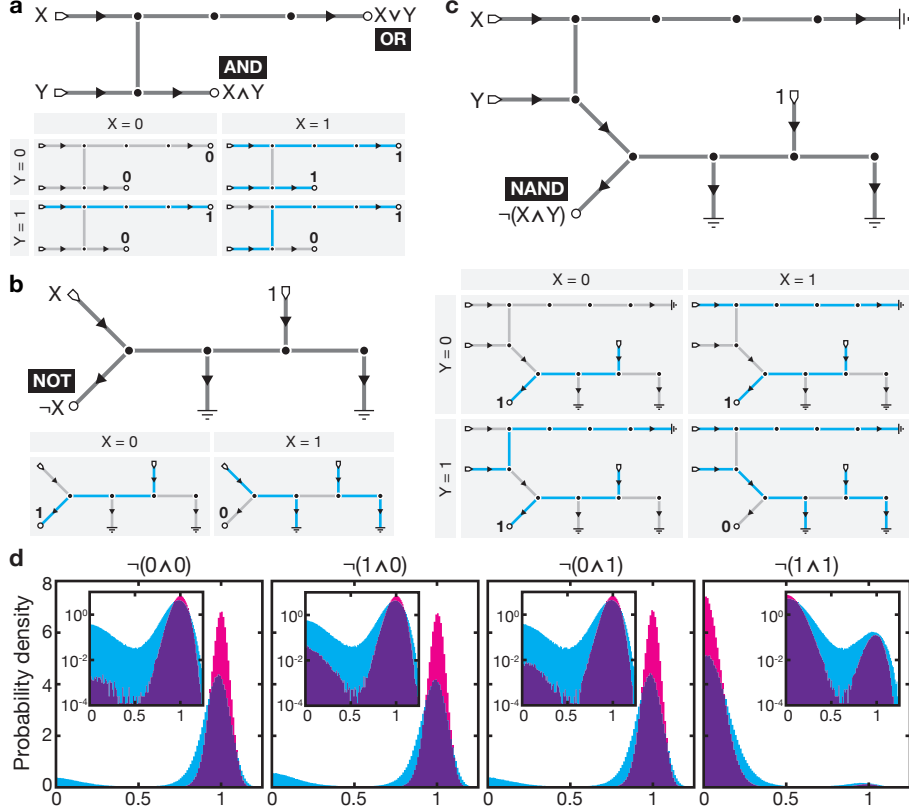


Figure 1 – Elementary logical operations realized with AFNs. **a**, An AFN whose ground states yield a simultaneous AND/OR gate. Either leg can be picked as the output depending on the operation desired, with the other sent to ground; alternatively, both could be used. Ground states for the four possible input combinations shown below, with active edges highlighted cyan. **b**, Logical NOT can be realized by a powered gate with two ground legs, as required by mass conservation. **c**, The NOT gate in **b** can be appended to the AND leg of **a** to yield NAND, provided the ground (OR) leg of **a** is lengthened to preserve the desired network states. **d**, Output histograms of the NAND gate in **c** at non-zero noise amplitudes, with $\beta\lambda = 100$ (magenta) and $\beta\lambda = 50$ (cyan); incompressibility is fixed at $\beta\mu = 500$ in both. Each histogram comprises 8×10^5 data points. Inset: histograms with log-scaled vertical axis.

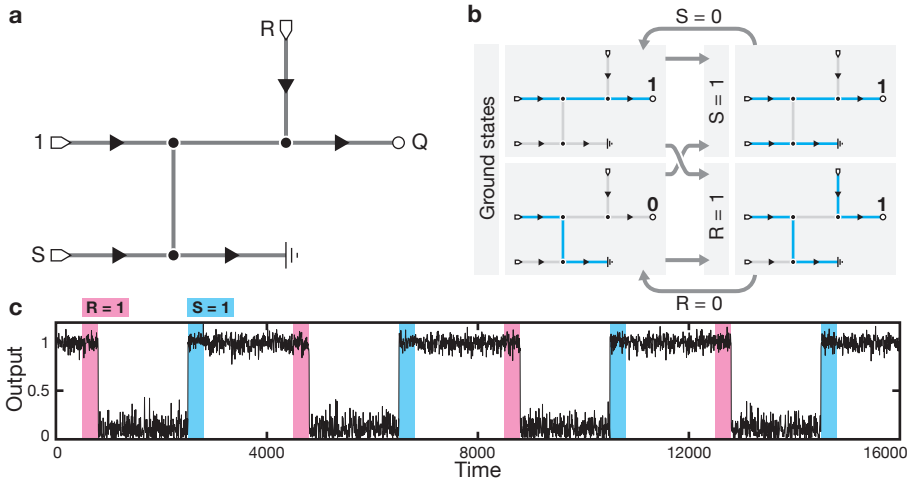


Figure 2 – Intrinsic multi-stability of AFNs allows the simple construction of a 1-bit memory circuit. **a**, AFN for a circuit with SR latch-like behavior. S and R are set and reset inputs, respectively, used to control the network output Q . **b**, With $S = R = 0$, the network has two ground states corresponding to $Q = 0$ and $Q = 1$. Raising to $S = 1$ forces an output of 1, which is maintained when S is released with high probability. Conversely, pulsing $R = 1$ forces the system into the output 0 ground state after R is released. Mass conservation means that $Q = 1$ while $R = 1$; traditional SR latch behavior could be achieved with an additional ground leg at the expense of network complexity. **c**, With low but non-zero noise, simulation of the network Langevin dynamics at $\beta\lambda = 100$, $\beta\mu = 500$ demonstrates the robust set–reset behavior of the network.

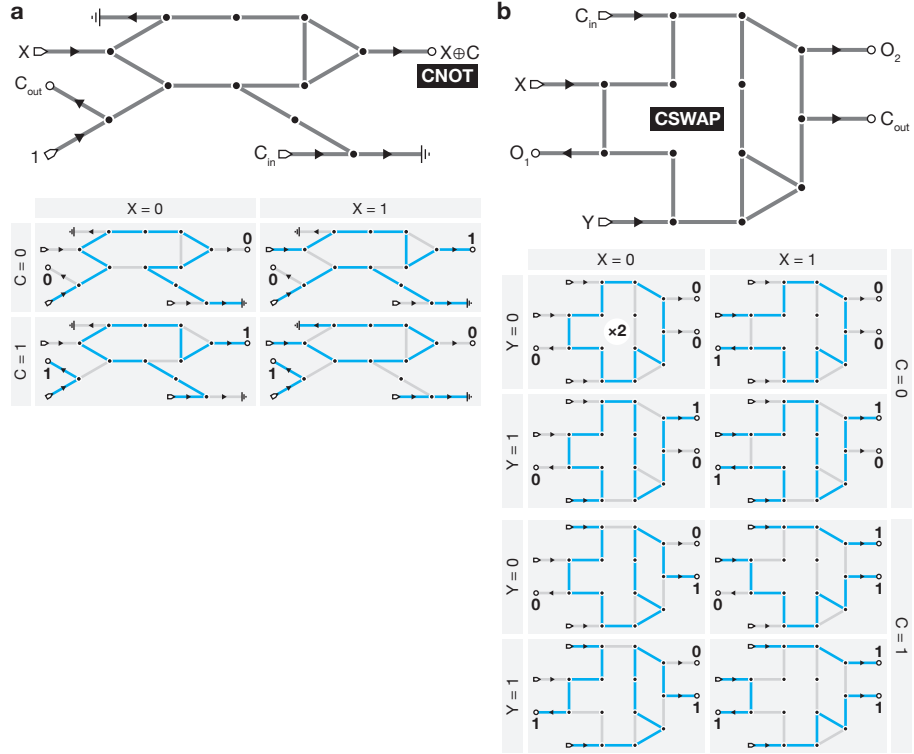


Figure 3 – Reversible gates can be realized through AFNs employing cycles in their topology. **a**, A CNOT gate, which provides a reversible XOR, and its ground states. Though C_{out} always equals C_{in} , it is not one flow path connecting the two. Instead, flow interactions mean that C_{out} is drawn from the power leg. **b**, A Fredkin gate, or CSWAP, and its ground states. If $C_{in} = 0$, then $O_1 = X$ and $O_2 = Y$; if $C_{in} = 1$, then $O_1 = Y$ and $O_2 = X$. Since AML is conservative, this gate needs no power or ground legs. Note that the all-zero input state has two ground states corresponding to clockwise and counterclockwise orientations of the flow loop. The gate implementations in **a** and **b** were determined by an exhaustive numerical ground state search over constrained random graphs.

References

- [1] Ge, Q., Qi, H. J. & Dunn, M. L. Active materials by four-dimension printing. *Appl. Phys. Lett.* **103** (2013).
- [2] Marchetti, M. C. *et al.* Hydrodynamics of soft active matter. *Rev. Mod. Phys.* **85**, 1143 (2013).
- [3] Din, M. O. *et al.* Synchronized cycles of bacterial lysis for in vivo delivery. *Nature* **536**, 81–85 (2016).
- [4] Tompkins, N. *et al.* Testing Turing’s theory of morphogenesis in chemical cells. *Proc. Natl. Acad. Sci. U.S.A.* **111**, 4397–4402 (2014).
- [5] Karzbrun, E., Tayar, A. M., Noireaux, V. & Bar-Ziv, R. H. Programmable on-chip DNA compartments as artificial cells. *Science* **345**, 829–832 (2014).
- [6] Langer, R. & Vacanti, J. P. Tissue engineering. *Science* **260**, 920–926 (1993).
- [7] Di Leonardo, R. *et al.* Bacterial ratchet motors. *Proc. Natl. Acad. Sci. U.S.A.* **107**, 9541–9545 (2010).
- [8] Thampi, S. P., Doostmohammadi, A., Shendruk, T. N., Golestanian, R. & Yeomans, J. M. Active micromachines: Microfluidics powered by mesoscale turbulence. *Sci. Adv.* **2**, e1501854 (2016).
- [9] Sanchez, T., Chen, D. T. N., DeCamp, S. J., Heymann, M. & Dogic, Z. Spontaneous motion in hierarchically assembled active matter. *Nature* **491**, 431 (2012).
- [10] Keber, F. C. *et al.* Topology and dynamics of active nematic vesicles. *Science* **345**, 1135–1139 (2014).
- [11] Thutupalli, S., Seemann, R. & Herminghaus, S. Swarming behavior of simple model squirmers. *New J. Phys.* **13**, 073021 (2011).
- [12] Walther, A. & Muller, A. H. E. Janus particles. *Soft Matter* **4**, 663–668 (2008).
- [13] Yan, J. *et al.* Reconfiguring active particles by electrostatic imbalance. *Nat. Mater.* **15**, 1095–1099 (2016).
- [14] Di Leonardo, R. Active colloids: Controlled collective motions. *Nat. Mater.* **15**, 1057–1058 (2016).
- [15] Bricard, A., Caussin, J.-B., Desreumaux, N., Dauchot, O. & Bartolo, D. Emergence of macroscopic directed motion in populations of motile colloids. *Nature* **503**, 95–98 (2013).
- [16] Sokolov, A. & Aranson, I. S. Physical properties of collective motion in suspensions of bacteria. *Phys. Rev. Lett.* **109**, 248109 (2012).
- [17] Wieland, H., Woodhouse, F. G., Dunkel, J. & Goldstein, R. E. Ferromagnetic and antiferromagnetic order in bacterial vortex lattices. *Nat. Phys.* **12**, 341–345 (2016).
- [18] Snejhko, A. & Aranson, I. S. Magnetic manipulation of self-assembled colloidal asters. *Nat. Mater.* **10**, 698–703 (2011).

[19] Wioland, H., Lushi, E. & Goldstein, R. E. Directed collective motion of bacteria under channel confinement. *New J. Phys.* **18**, 075002 (2016).

[20] Sokolov, A., Apodaca, M. M., Grzybowski, B. A. & Aranson, I. S. Swimming bacteria power microscopic gears. *Proc. Natl. Acad. Sci. U.S.A.* **107**, 969–974 (2010).

[21] Pearce, D. J. G. & Turner, M. S. Emergent behavioural phenotypes of swarming models revealed by mimicking a frustrated anti-ferromagnet. *J. R. Soc. Interface* **12** (2015).

[22] Nicolau Jr., D. V. *et al.* Parallel computation with molecular-motor-propelled agents in nanofabricated networks. *Proc. Natl. Acad. Sci. U.S.A.* **113**, 2591–2596 (2016).

[23] Wang, A. L. *et al.* Configurable NOR gate arrays from Belousov-Zhabotinsky micro-droplets. *Eur. Phys. J. Spec. Top.* **225**, 211–227 (2016).

[24] Tero, A. *et al.* Rules for biologically inspired adaptive network design. *Science* **327**, 439–442 (2010).

[25] Adamatzky, A. *Physarum Machines: Computers from Slime Molds* (World Scientific, Singapore, 2010).

[26] Prakash, M. & Gershenfeld, N. Microfluidic bubble logic. *Science* **315**, 832–835 (2007).

[27] Katsikis, G., Cybulski, J. S. & Prakash, M. Synchronous universal droplet logic and control. *Nat. Phys.* **11**, 588–596 (2015).

[28] Woodhouse, F. G., Forrow, A., Fawcett, J. B. & Dunkel, J. Stochastic cycle selection in active flow networks. *Proc. Natl. Acad. Sci. U.S.A.* **113**, 8200–8205 (2016).

[29] Sipser, M. *Introduction to the Theory of Computation* (Cengage Learning, Boston, USA, 2013), 3rd edn.

[30] Landauer, R. Irreversibility and heat generation in the computing process. *IBM J. Res. Develop.* **5**, 183–191 (1961).

[31] Berut, A. *et al.* Experimental verification of Landauer’s principle linking information and thermodynamics. *Nature* **483**, 187–189 (2012).

[32] Monroe, C., Meekhof, D. M., King, B. E., Itano, W. M. & Wineland, D. J. Demonstration of a fundamental quantum logic gate. *Phys. Rev. Lett.* **75**, 4714–4717 (1995).

[33] Hopfield, J. J. & Tank, D. W. Computing with neural circuits: A model. *Science* **223**, 625–633 (1986).

[34] Lestas, I., Vinnicombe, G. & Paulsson, J. Fundamental limits on the suppression of molecular fluctuations. *Nature* **467**, 174–178 (2010).

[35] Adleman, L. M. Molecular computation of solutions to combinatorial problems. *Science* **266**, 1021–1024 (1994).

[36] Lipton, R. J. DNA solution of hard computational problems. *Science* **268**, 542–545 (1996).

- [37] Hopfield, J. J. Neural networks and physical systems with emergent collective computational abilities. *Proc. Natl. Acad. Sci. U.S.A.* **79**, 2554–2558 (1982).
- [38] Denissenko, P., Kantsler, V., Smith, D. J. & Kirkman-Brown, J. Human spermatozoa migration in microchannels reveals boundary-following navigation. *Proc. Natl. Acad. Sci. U.S.A.* **109**, 8007–8010 (2012).
- [39] Fredkin, E. & Toffoli, T. Conservative logic. *Int. J. Theor. Phys.* **21**, 219–253 (1982).
- [40] Schneidman, E., Berry, M. J., Segev, R. & Bialek, W. Weak pairwise correlations imply strongly correlated network states in a neural population. *Nature* **440**, 1007–1012 (2006).
- [41] Schaller, V., Weber, C., Semmrich, C., Frey, E. & Bausch, A. R. Polar patterns of driven filaments. *Nature* **467**, 73–77 (2010).
- [42] Paoluzzi, M., Di Leonardo, R. & Angelani, L. Self-sustained density oscillations of swimming bacteria confined in microchambers. *Phys. Rev. Lett.* **115**, 188303 (2015).
- [43] Palacci, J., Sacanna, S., Steinberg, A. P., Pine, D. J. & Chaikin, P. M. Living crystals of light-activated colloidal surfers. *Science* **339**, 936–940 (2013).
- [44] Uspal, W. E., Popescu, M. N., Dietrich, S. & Tasinkevych, M. Guiding catalytically active particles with chemically patterned surfaces. *Phys. Rev. Lett.* **117**, 048002 (2016).